NASA/TM—2001-210815 FEDSM 2001–18134

Gust Acoustic Response of a Swept Rectilinear Cascade Using the Space-Time CE/SE Method

X.Y. Wang and A. Himansu
Taitech, Inc., Cleveland, Ohio

P.C. Jorgenson and S.C. Chang
Glenn Research Center, Cleveland, Ohio

Prepared for the
2001 Fluids Engineering Division Summer Meeting
sponsored by the American Society of Mechanical Engineers
New Orleans, Louisiana, May 29–June 1, 2001

National Aeronautics and
Space Administration

Glenn Research Center

April 2001

Acknowledgments

This work was supported by NASA Glenn Research Center through Contract NAS3-97186. The first author would like to thank Dr. Edmane Envia for his valuable help in this work.

Available from

NASA Center for Aerospace Information
7121 Standard Drive
Hanover, MD 21076
Price Code: A03

National Technical Information Service
5285 Port Royal Road
Springfield, VA 22100
Price Code: A03

Available electronically at http://gltrs.grc.nasa.gov/GLTRS

GUST ACOUSTIC RESPONSE OF A SWEPT RECTILINEAR CASCADE USING THE SPACE-TIME CE/SE METHOD

X.Y. Wang and A. Himansu
Taitech, Inc.
Cleveland, Ohio 44135

P.C. Jorgenson and S.C. Chang
National Aeronautics and Space Administration
Glenn Research Center
Cleveland, Ohio 44135

ABSTRACT

The benchmark problem 3 in Category 3 of the third Computational Aero-Acoustics (CAA) Workshop sponsored by NASA Glenn Research Center is solved using the space-time conservation element and solution element (CE/SE) method. This problem concerns the unsteady response of a rectilinear swept cascade to an incident gust. The acoustic field generated by the interaction of the gust with swept flat plates in the cascade is computed by solving the 3D nonlinear Euler equations using the space-time CE/SE method. A parallel version of the 3D CE/SE Euler solver is employed to obtain numerical solutions for several sweep angles. Numerical solutions are presented and compared with the analytical solutions.

INTRODUCTION

Fan noise is one of the dominant sources of engine noise on both takeoff and landing approach for turbofan engines with high bypass ratio. Thus the development of fan noise reduction technology is very important. Noise source control is one of the strategies to reduce the fan noise. One of the significant fan noise sources is the rotor-stator interaction noise. The fan (rotor) blades generate viscous wakes that appear as the periodic velocity fluctuations that are convected by the mean flow to interact with the downstream outlet guide vanes (stator), producing acoustic waves that propagate upstream and downstream. The benchmark problem 3 in Category 3 of the third CAA Workshop is a model problem of rotor-stator interaction noise. The gust represents the rotor viscous wake and the cascade of swept flat plates represents the stator. The effect of the sweep angle of the flat plate on the upstream radiated noise is investigated.

This benchmark problem is solved numerically by solving the unsteady 3D Euler equations using the space-time conservation element and solution element (CE/SE) method. The CE/SE method is an innovative numerical method for solving conservation laws. This method is distinguished from other methods by its requirement that the fluxes be conserved in both space and time. Simplicity, generality and accuracy were the goals in the development of this method. Its salient properties are summarized briefly as follows. First, both local and global flux conservations are enforced in space and time instead of in space only. Second, all the dependent variables and their spatial derivatives are considered as individual unknowns to be solved for simultaneously at each grid point. Third, every CE/SE scheme is based upon a non-dissipative scheme with addition of fully controllable numerical dissipation. This results in very low numerical dissipation. Fourth, the flux-based specification of the CE/SE schemes gives rise in a natural fashion to a simple yet generally effective non-reflecting boundary condition which is an important issue in CAA. Some practical advantages of the CE/SE method over the high order finite difference methods are summarized as follows: 1) it can handle both shocks and acoustic waves concurrently, 2) it can use both structured and unstructured meshes in one single algorithm to handle complex geometries, 3) it can avoid singular points without using any special treatment, 4) it has the most compact stencil, this leads to efficient parallel computing and easy implementation of boundary conditions, and 5) it can capture shocks accurately without using Riemann solvers or dimensional-splitting techniques.

A detailed description of this method and accompanying analysis can be found in [1–5]. Applications of this method to CAA problems reveal that, on mesh sizes used in practice, the result is comparable to that obtained using high order compact difference schemes even though the current solver is only 2nd-order accurate [6-11]. Especially for the CAA benchmark problems involving both shocks and acoustic waves, the CE/SE method can produce accurate solutions with much less effort than the high order finite difference methods [10,11].

In this paper, a parallel version of the 3D CE/SE Euler solver is used to compute the acoustic field generated by the interaction of a gust with a rectilinear swept cascade, which is described as the benchmark problem in Category 3 of the third CAA Workshop [12]. Different sweep angles of flat plates in the range of $[0°, 30°]$ are studied to determine the upstream-radiated noise as a function of sweep angle at the specified frequency. The variation of RMS pressure at an upstream point with the sweep angle is plotted and compared with the analytical solution.

In the following, the description of the benchmark problem is given first, which is followed by the boundary and initial conditions used in the calculation, and numerical results and discussion.

GUST-CASCADE PROBLEM

Consider the rectilinear cascade of swept flat plates shown in Fig. 1. The x-axis is aligned with the chord of the airfoil, the y-axis is perpendicular to it and the z-axis is normal to the bounding walls. The normal distance between walls is $2.6c$, where c is the chord length of the flat plate. The gap-to-chord ratio, s/c, is 1.0. The sweep angle of the flat plate, denoted by θ, varies from 0° to 30°.

The mean flow is assumed to be uniform and aligned with the x-axis. The mean flow variables are inflow velocity, U_0, static density, ρ_0, and static pressure, p_0. The inflow Mach number, M_0, is 0.5. Flow variables are nondimensionalized by using a_0(the speed of sound) as the velocity scale, c as the length scale, c/a_0 as the time scale, ρ_0 as the density scale and $\rho_0 a_0^2$ as the pressure scale. Thus the mean flow is described in dimensionless variables as

$$\rho = 1, \quad u = 0.5, \quad v = 0, \quad w = 0, \quad p = 1.0/1.4 \qquad (1)$$

The incident gust carried by the mean flow has x, y, and z velocity components given by

$$u' = -(v_G k_y/k_x)\cos(k_x x + k_y y + k_z z - \omega t) \qquad (2)$$

and

$$v' = v_G \cos(k_x x + k_y y + k_z z - \omega t), \quad w' = 0 \qquad (3)$$

respectively, where $v_G = 0.0001$ and $k_x = 5.5, k_y = \pi, k_z = 0$, and $\omega = M_0 k_x$, respectively. The corresponding period of the gust wave is $T = 2\pi/\omega$. It is assumed that the gust is "frozen" and convected by the uniform mean flow. Thus the gust satisfies the linearized Euler equations. This implies that $\rho' = p' = 0$. The gust is continually convected from the inlet by the mean flow and will interact with the swept flat plates to generate acoustic waves. The whole flow field, including the acoustics, gust wave and mean flow, is simulated by solving the nonlinear Euler equations.

BOUNDARY AND INITIAL CONDITIONS

Having the gust superposed on the mean flow, the flow properties at the inlet are described as:

$$(u_1)_j^n = \rho \qquad (4)$$
$$(u_2)_j^n = \rho(u + u') \qquad (5)$$
$$(u_3)_j^n = \rho(v + v') \qquad (6)$$
$$(u_4)_j^n = \rho(w + w') \qquad (7)$$
$$(u_5)_j^n = \frac{p}{\gamma - 1} + \frac{\rho}{2}[(u + u')^2 + (v + v')^2 + (w + w')^2] \qquad (8)$$

The inlet values of $(u_{mx})_j^n$, $(u_{my})_j^n$, and $(u_{mz})_j^n$ are obtained by evaluating derivatives of u_m at (j, n). This is one method for imposing the non-reflecting BC in the CE/SE method [6]. An alternative non-reflecting scheme is used at the outlet, as follows

$$(u_m)_j^{n+1} = (u_m)_{j-1}^{n+1/2}, \quad (u_{mx})_j^{n+1} = 0$$
$$(u_{my})_j^{n+1} = (u_{my})_{j-1}^{n+1/2}, \quad (u_{mz})_j^{n+1} = (u_{mz})_{j-1}^{n+1/2} \qquad (9)$$

This way of imposing the non-reflecting boundary conditions allows the flux to "stream" out of the spatial domain smoothly with minimal reflection. The periodic boundary condition is imposed on planes $y = -0.5$ and $y = 1.5$ and the reflecting boundary conditions are used on the flat plate surfaces and top and bottom walls in the z-coordinate direction. No grid points are located at the flat plate leading and trailing edges, in order to avoid the singular flow behavior.

At $t = 0$, the time-marching variables $(u_m)_j^n$ in the whole domain are defined using Eqs. (4)–(8) with $t = 0$, and $(u_{mx})_j^n, (u_{my})_j^n$, and $(u_{mz})_j^n$ are obtained by evaluating derivatives of u_m at (j, n).

NUMERICAL RESULTS AND DISCUSSION

A structured 291x21x27 hexahedral grid is generated by using an algebraic transformation in the computational domain of $-6 \le x \le 8.5$, $-0.5 \le y \le 1.5$, and $0 \le z \le 2.6$ first. A slice of the grid in x-z planes is shown in Fig. 2. Each hexahedron is cut into six tetrahedrons in the way shown in Fig. 3, which results in 904800 (290x20x26x6) tetrahedral cells in the computation. The parallel version of the 3D Euler solver is used with $\alpha = 0$ and $\epsilon = 0.5$, where α and ϵ are the parameters connected with the specification of the numerical dissipation in the solver [4]. A detailed description of the 3D Euler solver is referred to in [4] and the parallelization part is given in [5]. For $\theta \le 25^\circ$, $\Delta t = T/168$, while $\Delta t = T/200$ for $\theta = 30^\circ$.

The sweep angle of flat plates is varied to determine its effect on the upstream-radiated noise level. Sweep angles in the range of $[0^\circ, 30^\circ]$ are studied here. In all figures, the acoustic pressure p' non-dimensionalized by v_G is plotted. The time history of the acoustic pressure at an upstream point located at around $(-5, 0, 1.3)$ is shown in Fig. 4 for sweep angles in the range of $[2^\circ, 30^\circ]$. It should be pointed out that numerical instability arises at leading edge with the current meshing strategy shown in Fig. 3 for sweep angles that are less than 5°. No converged solution is obtained for $\theta = 0^\circ$. Some instabilities are observed for $\theta = 2^\circ$. This instability can be overcome by using a different meshing strategy, such as cutting each hexahedron into 24 tetrahedrons through diagonal lines, which is not presented here. It can be seen that the solution is fully converged for $\theta \ge 5^\circ$ by $t = 46T = 105.1$. And the absolute amplitude of the acoustic pressure at the upstream decreases when the sweep angle increases.

The numerical result of the RMS pressure at the upstream point needs to be expressed in dB using the value for $\theta = 0^\circ$ as the reference. However, the computed result of the RMS pressure for $\theta = 0^\circ$ is not available. Thus the value of the RMS pressure for $\theta = 5^\circ$ is used as the reference with a correction such that the value of the computed dB pressure is identical to the analytical solution for $\theta = 5^\circ$. The so-obtained data is plotted in Fig. 5 along with the analytical solution [13] that shows the upstream-radiated noise level is reduced substantially by increasing the sweep angle, and the noise field is cut-off at the critical sweep angle. A reasonable agreement between numerical and analytical solutions is observed for smaller sweep angles ($\le 15^\circ$), while there are significant discrepancies for larger sweep angles ($\ge 20^\circ$). One possible explanation is that the effect of the 3D corners formed by the upper (lower) wall and the flat plates becomes significant for larger sweep angles. However, the 3D corner effect is not fully taken into account in the analytical solution [14]. The numerical error caused by the reflection at the outlet is investigated by running the code in a smaller domain. A similar grid of 201x21x27 in a domain of $-6 \le x \le 4$, $-0.5 \le x \le 1.5$, and $0 \le z \le 2.6$ is used with the identical boundary conditions. The corresponding data is plotted for $\theta = 5^\circ, 10^\circ$, and 15° in Fig. 6. As expected, a slightly better result is produced by using the larger domain. The solutions obtained using two different domains are very close, which means the boundary condition has small effect on the accuracy of numerical solutions.

Further, the acoustic pressure contours on the upper and lower surfaces of the flat plate are plotted in Fig. 7 for several sweep angles to show the different wave patterns near the noise source. The pressure contours on x-y and y-z planes and pressure distribution at some constant lines are shown in Figs. 8–9 for two sweep angles. It can be seen that the variation of the acoustic field in the z- direction is amplified by increasing the sweep angle and the solutions show the periodicity at the periodic boundary.

The parallel 3D CE/SE code was run on Origin2000 clusters. For a mesh of 904800 cells, it takes around 5 hrs of wall-clock time to reach $t = 46T$ (15456 time iterations) using 31 CPUs.

CONCLUSION

The problem 3 in Category 3 of the third CAA Workshop has been solved by using the 3D parallel CE/SE Euler solver. Numerical results are presented for several sweep angles. The result of the RMS pressure at an upstream point is compared with the analytical solution, showing a reasonable agreement for smaller sweep angles ($\le 15^\circ$).

REFERENCES

[1] S.C. Chang, "The Method of Space-Time Conservation Element and Solution Element – A New Approach for Solving the Navier-Stokes and Euler Equations," *J. Comput. Phys.*, **119,** pp. 295-324, (1995).

[2] S.C. Chang, X.Y. Wang, and C.Y. Chow, "The Space-Time Conservation Element and Solution Element Method – A New High-Resolution and Genuinely Multidimensional Paradigm for Solving Conservation Laws," *J. Comput. Phys.*, **156,** pp. 89–136, (1999).

[3] X.Y. Wang and S.C. Chang, "A 2D Non-splitting Unstructured-triangular-mesh Euler Solver based on the

Method of Space-Time Conservation Element and Solution Element," Vol. 8, No. 2, pp. 326-340, 1999, *Computational Fluid Dynamics JOURNAL*.
[4] X.Y. Wang and S.C. Chang, "A 3D Non-splitting Structured/Unstructured Euler Solver based on the Method of Space-Time Conservation Element and Solution Element," AIAA Paper 98-3278, Norfolk, Virginia, June, 1998.
[5] A. Himansu, P. Jorgenson, X.Y. Wang and S.C. Chang, "Parallel CE/SE Computations via Domain Decomposition," in the proceeding of 1st International Conference of Computational Fluid Dynamics, Kyoto, June, 2000.
[6] S.C. Chang, A. Himansu, C.Y. Loh, X.Y. Wang, S.T. Yu and P.C.E. Jorgenson, "Robust and Simple Non-Reflecting Boundary Conditions for the Space-Time Conservation Element and Solution Element Method," AIAA Paper 97-2077, June 29-July 2, 1997, Snowmass, CO.
[7] C.Y. Loh, S.C. Chang, J.R. Scott and S.T. Yu, "The Space-Time Conservation Element Method – A New Numerical Scheme for Computational Aeroacoustics," AIAA Paper 96-0276, January 15-18, 1996, Reno, NV.
[8] C.Y. Loh, L.S. Hultgren and S.C. Chang, "Computing Waves in Compressible Flow Using the Space-Time Conservation Element and Solution Element method," AIAA Paper 98-0369, January 12-15, 1998, Reno, NV.
[9] X.Y. Wang, C.Y. Chow and S.C. Chang, "Numerical Simulation of Gust Generated Aeroacoustics in a Cascade Using the Space-Time Conservation Element and Solution Element Method," AIAA Paper 98-0178, January 12-15, 1998, Reno, NV.
[10] X.Y. Wang, S.C. Chang, and P. Jorgenson, "Prediction of Sound Waves Propagating through a Nozzle without/with a Shock Wave Using the Space-Time CE/SE Method," AIAA 2000-0222, Reno, NV, January, 2000.
[11] X.Y. Wang, S.C. Chang, and P. Jorgenson, "Accuracy Study of the Space-Time CE/SE Method for Computational Aeroacoustics Problems Involving Shock Waves," AIAA 2000-0474, Reno, NV, January, 2000.
[12] The Proceeding of the Third Computational Aeroacoustics (CAA) Workshop on Benchmark Problems, November 8–10, 1999, Cleveland, Ohio.
[13] E. Envia and E. Kerschen, "Influence of Vane Sweep on Rotor-Stator Interaction Noise," NASA Contractor Report 187052, December 1990.
[14] Private communication with Dr. Edmane Envia.

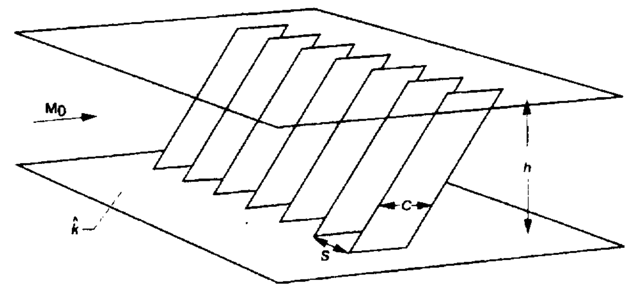

Figure 1. GEOMETRY OF SWEPT RECTILINEAR CASCADE IN A FINITE DOMAIN.

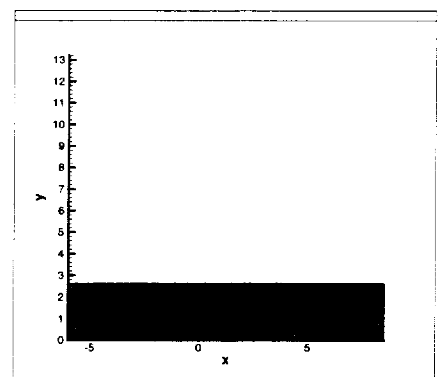

Figure 2. A SLICE OF THE HEXAHEDRAL MESH ON THE X-Z PLANE.

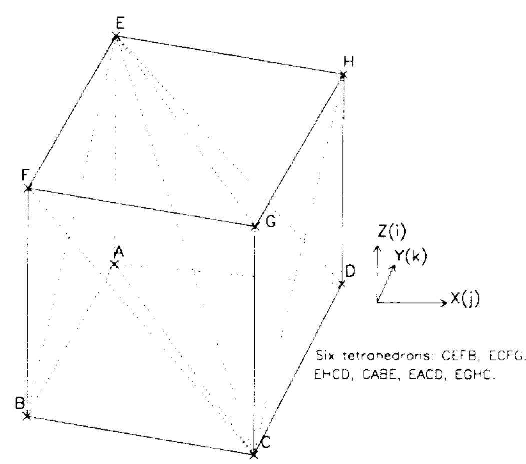

Figure 3. SIX TETRAHEDRONS IN EACH HEXAHEDRON.

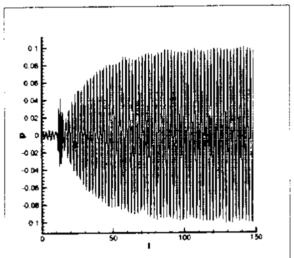

(1) $\theta = 2°$.

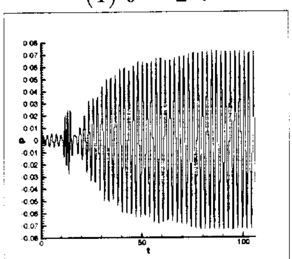

(2) $\theta = 5°$.

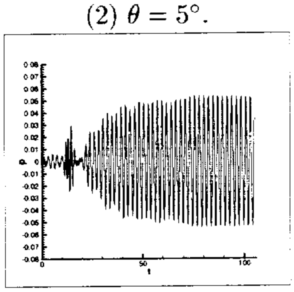

(3) $\theta = 7.5°$.

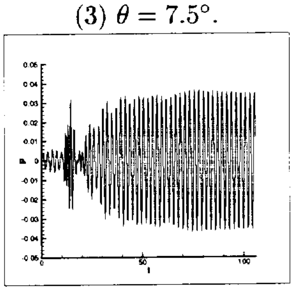

(4) $\theta = 10°$.

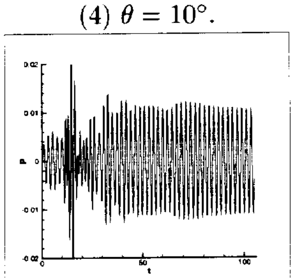

(5) $\theta = 15°$.

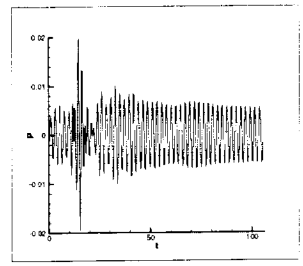

(6) $\theta = 17.5°$.

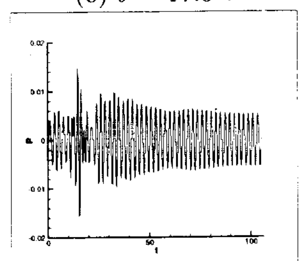

(7) $\theta = 20°$.

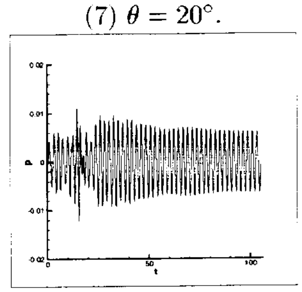

(8) $\theta = 22.5°$.

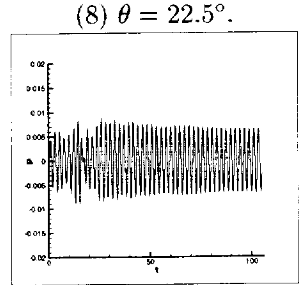

(9) $\theta = 25°$.

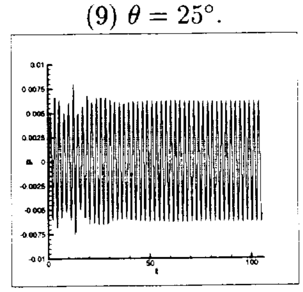

(10) $\theta = 30°$.

Figure 4. TIME HISTORY OF THE ACOUSTIC PRESSURE AT AN UPSTREAM POINT LOCATED AT $(-5, 0, 1.3)$ FOR DIFFERENT SWEEP ANGLES.

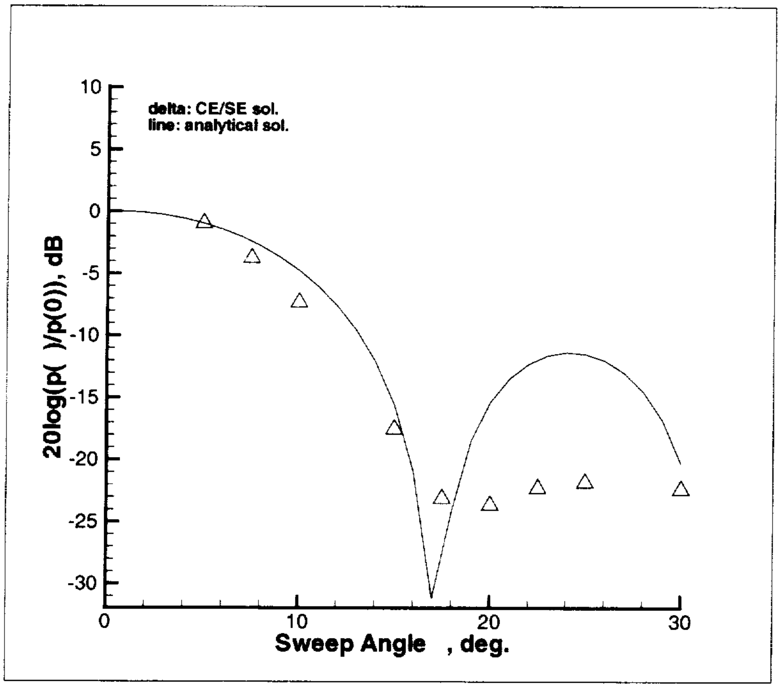

Figure 5. THE dB PRESSURE AT AN UPSTREAM POINT LOCATED AT $(-5, 0, 1.3)$ VERSUS THE SWEEP ANGLE θ.

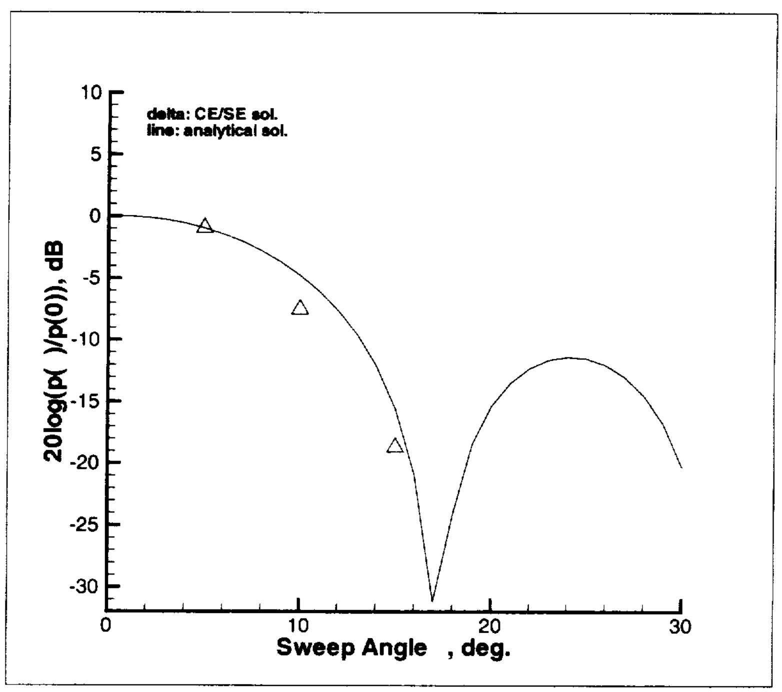

Figure 6. THE dB PRESSURE AT AN UPSTREAM POINT LOCATED AT $(-5, 0, 1.3)$ VERSUS THE SWEEP ANGLES IN A SMALLER COMPUTATIONAL DOMAIN.

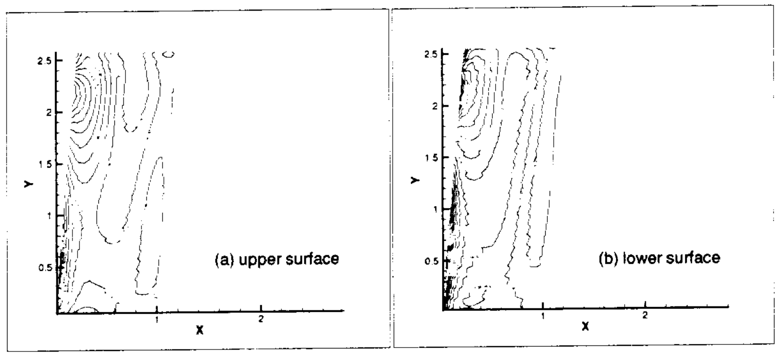

(1) $\theta = 5°$.

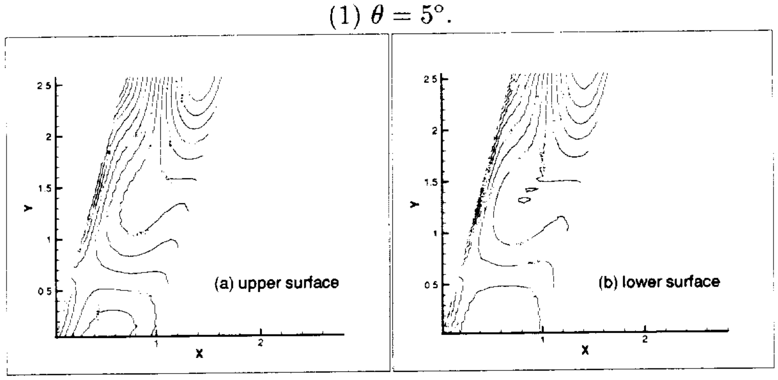

(2) $\theta = 15°$.

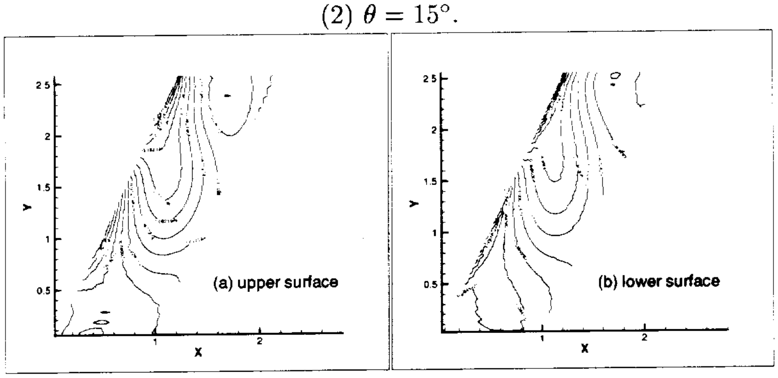

(3) $\theta = 25°$.

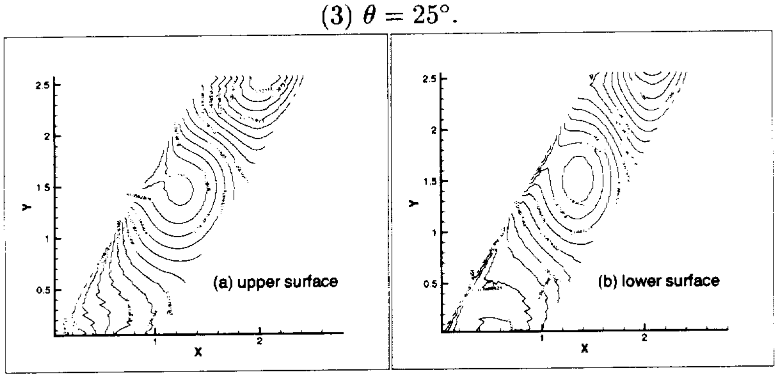

(4) $\theta = 30°$.

Figure 7. ACOUSTIC PRESSURE CONTOUR ON THE BLADE SURFACES AT $t = 46T$ FOR DIFFERENT SWEEP ANGLES.

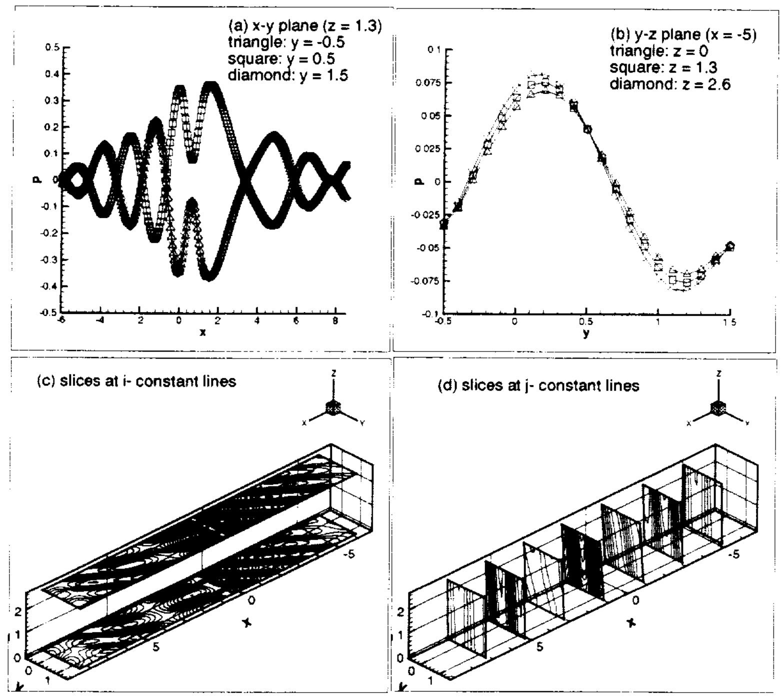

Figure 8. ACOUSTIC PRESSURE CONTOURS AND DISTRIBUTION ON $X-Y$ AND $Y-Z$ PLANES FOR $\theta = 5°$.

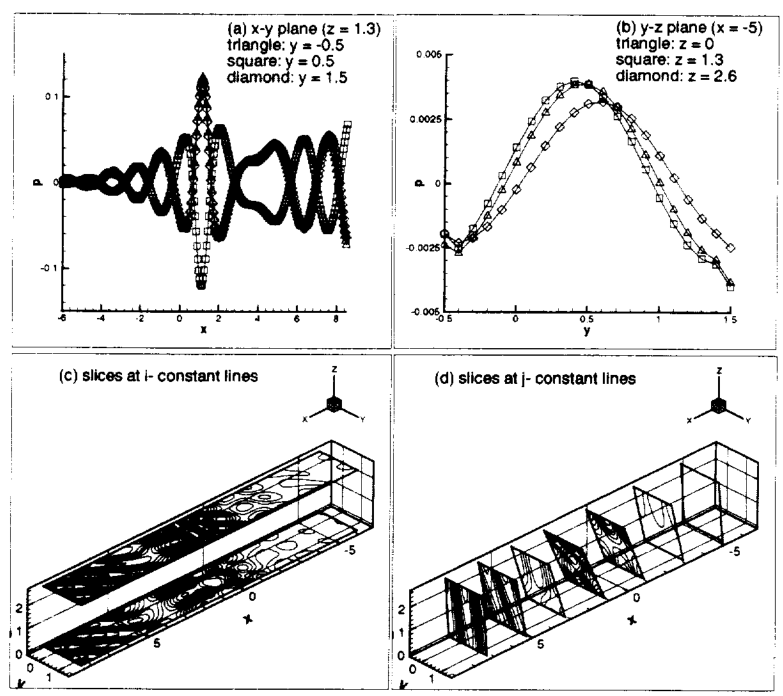

Figure 9. ACOUSTIC PRESSURE CONTOURS AND DISTRIBUTION ON $X-Y$ AND $Y-Z$ PLANES FOR $\theta = 25°$.

REPORT DOCUMENTATION PAGE			Form Approved OMB No. 0704-0188

1. AGENCY USE ONLY (*Leave blank*)	2. REPORT DATE	3. REPORT TYPE AND DATES COVERED
	April 2001	Technical Memorandum

4. TITLE AND SUBTITLE

Gust Acoustic Response of a Swept Rectilinear Cascade Using the Space-Time CE/SE Method

5. FUNDING NUMBERS

WU–708–90–43–00

6. AUTHOR(S)

X.Y. Wang, A. Himansu, P.C. Jorgenson, and S.C. Chang

7. PERFORMING ORGANIZATION NAME(S) AND ADDRESS(ES)

National Aeronautics and Space Administration
John H. Glenn Research Center at Lewis Field
Cleveland, Ohio 44135–3191

8. PERFORMING ORGANIZATION REPORT NUMBER

E–12730

9. SPONSORING/MONITORING AGENCY NAME(S) AND ADDRESS(ES)

National Aeronautics and Space Administration
Washington, DC 20546–0001

10. SPONSORING/MONITORING AGENCY REPORT NUMBER

NASA TM—2001-210815
FEDSM 2001–18134

11. SUPPLEMENTARY NOTES

Prepared for the 2001 Fluids Engineering Division Summer Meeting sponsored by the American Society of Mechanical Engineers, New Orleans, Louisiana, May 29–June 1, 2001. X.Y. Wang and A. Himansu, Taitech, Inc., 21000 Brookpark, Road, Cleveland, Ohio 44135; P.C. Jorgenson and S.C. Chang, NASA Glenn Research Center. Responsible person, Richard A. Blech, organization 5880, 216–433–3657.

12a. DISTRIBUTION/AVAILABILITY STATEMENT

Unclassified - Unlimited
Subject Categories: 34 and 07 Distribution: Nonstandard

Available electronically at http://gltrs.grc.nasa.gov/GLTRS

This publication is available from the NASA Center for AeroSpace Information, 301–621–0390.

12b. DISTRIBUTION CODE

13. ABSTRACT ***(Maximum 200 words)***

The benchmark problem 3 in Category 3 of the third Computational Aero-Acoustics (CAA) Workshop sponsored by NASA Glenn Research Center is solved using the space-time conservation element and solution element (CE/SE) method. This problem concerns the unsteady response of a rectilinear swept cascade to an incident gust. The acoustic field generated by the interaction of the gust with swept at plates in the cascade is computed by solving the 3D nonlinear Euler equations using the space-time CE/SE method. A parallel version of the 3D CE/SE Euler solver is employed to obtain numerical solutions for several sweep angles. Numerical solutions are presented and compared with the analytical solutions.

14. SUBJECT TERMS

Computational aeroacoustics; Turbomachinery

15. NUMBER OF PAGES	16. PRICE CODE
14	A03

17. SECURITY CLASSIFICATION OF REPORT	18. SECURITY CLASSIFICATION OF THIS PAGE	19. SECURITY CLASSIFICATION OF ABSTRACT	20. LIMITATION OF ABSTRACT
Unclassified	Unclassified	Unclassified	